PHYSICAL REVIEW E, VOLUME 64, 045204(R)

Critical states and fractal attractors in fractal tongues: Localization in the Harper map

Surendra Singh Negi and Ramakrishna Ramaswamy
School of Physical Sciences, Jawaharlal Nehru University, New Delhi 110 067, India
(Received 12 April 2000; revised manuscript received 31 August 2000; published 21 September 2001)

Localized states of Harper's equation correspond to strange nonchaotic attractors in the related Harper mapping. In parameter space, these fractal attractors with nonpositive Lyapunov exponents occur in fractally organized tongue-like regions which emanate from the Cantor set of eigenvalues on the critical line $\epsilon=1$. A topological invariant characterizes wave functions corresponding to energies in the gaps in the spectrum. This permits a unique integer labeling of the gaps and also determines their scaling properties as a function of potential strength.

DOI: 10.1103/PhysRevE.64.045204 PACS number(s): 05.45.Mt, 05.45.Df, 71.23.An, 75.30.Kz

The Harper equation [1],

$$\psi_{n+1}+\psi_{n-1}+V(n)\psi_n=E\psi_n, \tag{1}$$

where ψ_n denotes the wave function at lattice site n, and $V(n)=2\epsilon\cos 2\pi(n\omega+\phi_0)$ with ω irrational, has been extensively studied in the context of localization. This discrete Schrödinger equation for a particle in a quasiperiodic potential on a lattice, arises in a number of different problems [2,3]. It is known [4] that the eigenstates can be extended ($\epsilon<1$), localized ($\epsilon>1$), or critical ($\epsilon=1\equiv\epsilon_c$), when the eigenvalue spectrum is singular-continuous [5], and the states are power-law localized [6]. Renormalization group studies [7–9] of this model have been very effective in establishing the multifractal nature of the wave functions of such states and of the eigenvalue spectrum [10].

Through the transformation $\psi_{n-1}/\psi_n\rightarrow x_n$, Eq. (1) reduces to the (equivalent) Harper map [11]

$$x_{n+1}=-[x_n-E+2\epsilon\cos 2\pi\phi_n]^{-1}, \tag{2}$$

$$\phi_{n+1}=\{\omega+\phi_n\}, \tag{3}$$

where $\{y\}\equiv y \bmod 1$, and n is now the time or iteration index. Viewed as a skew-product dynamical system, this is now a driven mapping of the infinite strip $(-\infty,\infty)\otimes[0,1]$ to itself. Irrational ω implies that the forcing in Eq. (2) is quasiperiodic.

The Harper map, which we study in this Rapid Communication, provides an alternate means of analyzing the eigenvalue spectrum of the Harper equation. Boundary conditions that must be imposed on Eq. (1) in order to determine eigenstates become conditions on the dynamical states in the map, Eqs. (2) and (3), where E now appears as a parameter. Although there is no chaotic motion since the map is reversible, for large enough ϵ, the attractor of the dynamics is a fractal [11]. On this attractor, the dynamics is nonchaotic [12]: these are therefore strange nonchaotic attractors (SNAs) [13] that are generic in quasiperiodically forced systems. There are no periodic orbits, but there can be a variety of other nonfractal quasiperiodic (torus) attractors.

When E is an eigenvalue, a correspondence relates localized states of the quantum problem to SNAs in the associated map, an equivalence first noted by by Bondeson, Ott, and Antonsen [14] in a study of the continuous version of the same problem. The wave functions for critical and extended states have a quasiperiodic symmetry [12], while the fractal fluctuations of the amplitudes of the localized states [9] appear as fractal density fluctuations in the attractors of the map. The nontrivial Lyapunov exponent of the system is given by $\lambda=\lim_{N\rightarrow\infty}1/N\Sigma_{i=1}^{N}\ln x_{n+1}^2$. At ϵ_c, if E is an eigenvalue of the quantum problem, then this quantity is exactly zero [12]; see Fig. 1. Above ϵ_c, the localization length for quantum states γ is inversely related to the Lyapunov exponent [4] $\lambda^{-1}=-\gamma/2$. Knowledge of this equivalence thus permits the complete determination of the quantum spectrum of the Harper system through a study of the Lyapunov exponents of the Harper map. At every eigenvalue (Fig. 1), there is a bifurcation from a quasiperiodic attractor to a SNA when the Lyapunov exponent becomes zero.

The spectrum of the Harper equation is invariant under the transformation $\omega\rightarrow 1-\omega$, and is symmetric about $E=0$, so it suffices to consider only positive eigenvalues and $\omega>1/2$. The behavior of the spectral *gaps* has been of considerable interest [3], and we study this here by describing the phase diagram of this system for $\omega=\omega_g=(\sqrt{5}-1)/2$, the inverse golden-mean ratio.

At $\epsilon=0$, the states of the quantum system form a band between energies $0\leqslant E\leqslant 2$. As ϵ is increased, the gaps open up and merge as $\epsilon\rightarrow\epsilon_c$, giving a singular continuous spec-

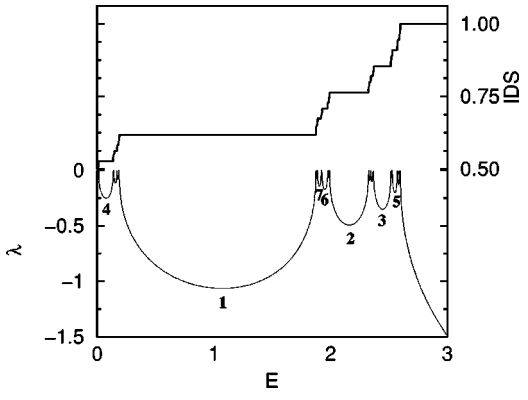

FIG. 1. The integrated density of states (IDS) (scale on the right) and Lyapunov exponent (λ) (scale on the left) versus energy at ϵ_c. The gap labels k are indicated for the largest visible gaps. At every bifurcation, when $\lambda=0$, the dynamics is on a SNA. On the gaps, the IDS takes the constant value Ω_k, specified by Eq. (4).

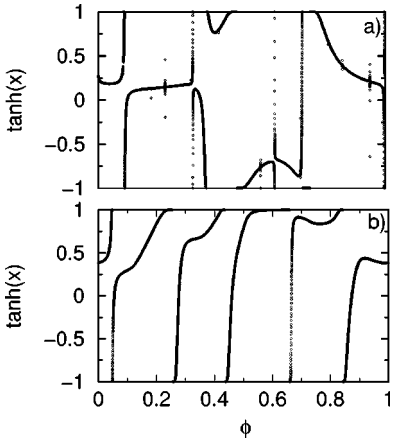

FIG. 2. (a) A strange nonchaotic attractor for $\epsilon=2$, $E=3$. (b) The attractor for a value of E corresponding to the gap $N=5$, having five branches that traverse the range $-\infty<x<\infty$.

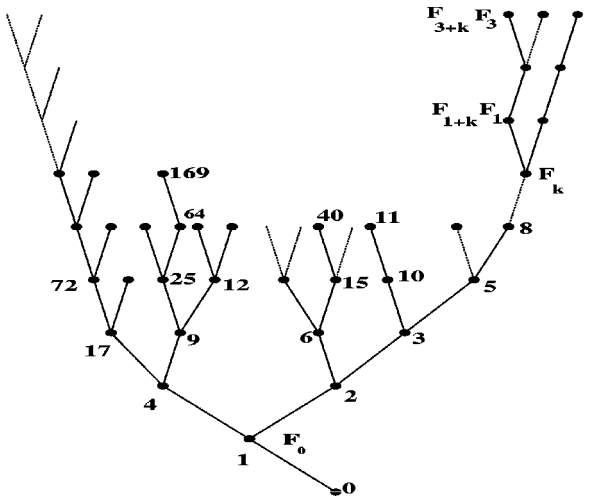

FIG. 3. Ordering of the gaps for $\omega=\omega_g$ the golden mean. Only part of the Cayley tree described in the text is shown for clarity. Each node has two daughters except for the root 0.

trum. Below ϵ_c, when the states are extended, the dynamics of the classical system is on ''three-frequency'' quasiperiodic orbits [14] with the Lyapunov exponent equal to 0. Above ϵ_c, localized states correspond to SNAs with a negative Lyapunov exponent [see Fig. 2(a) for an example], while critically localized states at ϵ_c are exceptional and correspond to SNAs with a zero Lyapunov exponent [12]. For energies in the gaps, $\lambda<0$, and the motion is on two-frequency quasiperiodic (one-dimensional) attractors [an example is shown in Fig. 2(b)], which wind across the (x,θ) plane an integral number of times. Wave functions of Eq. (1) at these energies do not satisfy the appropriate boundary conditions and are non-normalizable. The number of windings of the corresponding attractor N is a topological invariant for *all* orbits in the gaps. This integer index for each gap [15] counts the number of changes of sign (per unit length) of the wave function, and is thus related to the integrated density of states (IDS) [16]. The gap-labeling theorem [16] states that each gap can be labeled by the value that the IDS takes on the gap; in the Harper system, this is also the winding number [15], and (for $E\geqslant 0$) on the gap labeled by the index N, this takes the value

$$\Omega_N(E)=\max(\{N\omega\},1-\{N\omega\}). \tag{4}$$

The symmetrically located gap with $E\leqslant 0$ with index N has the winding number $\Omega_N(E)=\min(\{N\omega\},1-\{N\omega\})$.

There is thus a 1–1 correspondence between the gaps and the integers. Furthermore, since the IDS is a continuous nondecreasing curve, it is possible to specify the gap ordering: this depends on the continued fraction representation of ω. This latter problem earlier studied by Slater [17], is also encountered in the context of level statistics of two-dimensional harmonic oscillator systems [18]. Consider the numbers $y_j=\{j\omega\}, j=1,2,\ldots,m$. For *any* ω and any m, it has been shown [17,18] that an ''ordering function'' can be defined, giving a permutation of the indices, $j_1,j_2,\ldots,j_m$, such that $y_{j_i}\leqslant y_{j_k}$ if $i<k$. This result can be directly adapted to the present problem to give the complete ordering of gap labels with E [19].

The resulting structure of the gaps can be described via a simpler construction for the case of $\omega=\omega_g \equiv \lim_{k\to\infty} F_{k-1}/F_k$, where the Fibonacci numbers F_k are defined by the recursion $F_{k+1}=F_{k-1}+F_k$, with $F_0=1, F_1=2$. Consider a Cayley tree, shown in Fig. 3, rooted at the origin which is labeled 0. Nodes at the same horizontal level are at the same generation. The rightmost node at each generation is labeled by successive Fibonacci integers, while the leftmost are half the successive even Fibonacci integers. For a given non-Fibonacci number m, the parent node i_m is the smallest available such that the sum (i_m+m) is a Fibonacci number. Subsidiary number-theoretic properties help in determining the placement of all integers on the tree.

Every pair of integers, i_1 and i_2, with $i_2>i_1$, has two possibilities as to how they are relatively placed on this graph. Either (i) i_1 is an ancestor of i_2, i.e., there is a directed path connecting i_2 to i_1. If this path is to the left at node i_1, then $i_2<i_1$. (If to the right, then $i_1<i_2$.) or (ii) i_0 is the most recent common ancestor of i_1 and i_2. If the path from i_0 to i_1 is on the left at i_0, then $i_1<i_2$. (Similarly, if it is to the right, then $i_2<i_1$.)

This gives a unique ordering of the integers (see Fig. 3) with the relation $\prec$ being transitive (if $i\prec j$ and $j\prec m$ then $i\prec m$),

$$\ldots 4\prec\ldots\prec 9\prec\ldots\prec 1\prec 2\prec\ldots\prec 11\prec\ldots\prec 0.$$

The gaps appear in *precisely* this order: if $k\prec k'$, then gap k precedes gap k' in the positive energy spectrum of the critical Harper map [Fig. 1]. Following the procedure that is described in detail in [18], similar Cayley trees can be constructed for any other irrational frequency. For each ω, depending on its continued fraction representation, there is a unique reordering of the integers corresponding to the ordering of the gaps.

Each gap is characterized by its width w_m and by its depth d_m, both of which are functions of ϵ. The depth has no obvious quantum-mechanical interpretation, $-d_m$ merely be-

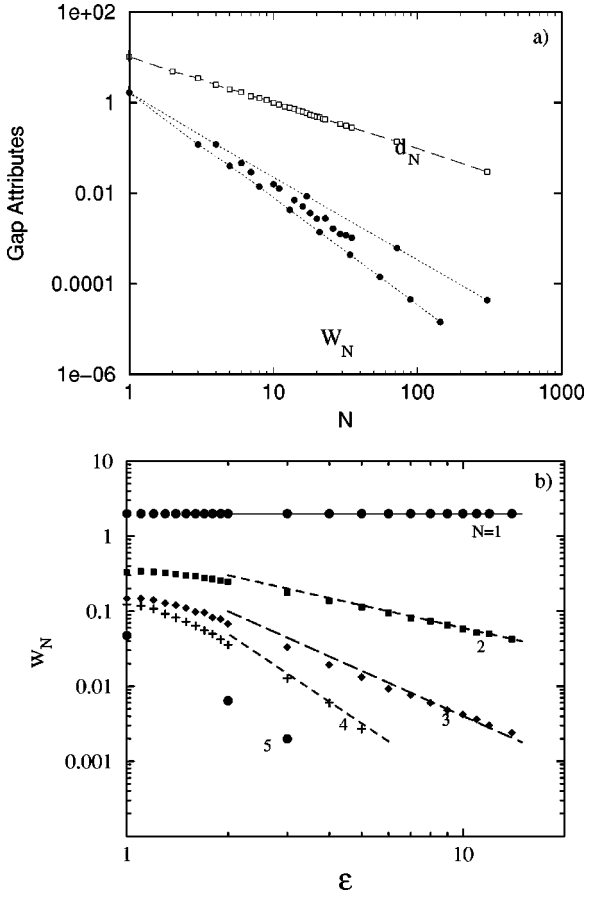

FIG. 4. (a) Scaling of the gap widths, w_N (●), and depths d_N (◇), as a function of gap index N at $\epsilon = \epsilon_c$. The depths have been multiplied by a factor of 10 for clarity, and the dashed line has slope -1. The dotted lines show the scaling of the widths for two families of gaps; see the text for details. (b) Scaling of the gap widths w_N for the largest few gaps as a function of ϵ above ϵ_c. The solid lines are the power laws given in Eq. (5).

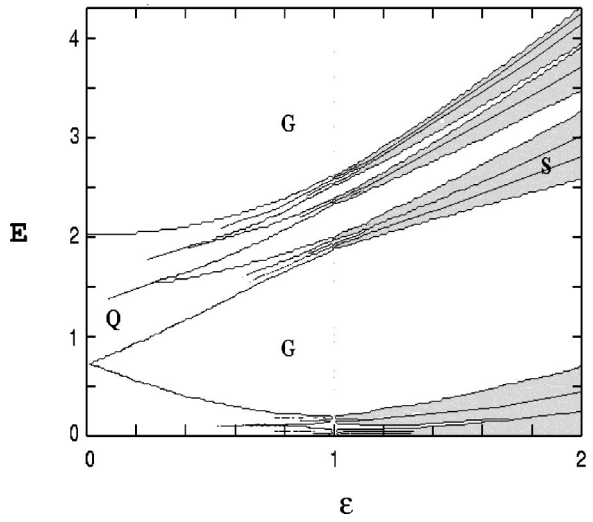

FIG. 5. Phase diagram for the Harper map. Below ϵ_c (the dotted vertical line) there are three-frequency quasiperiodic (Q) orbits or extended states, 1-d attractors or gaps (G), and above ϵ_c, SNAs (S) and gaps (G). Only the largest gaps are visible at this scale. All gaps persist above ϵ_c, decreasing in width according to Eq. (5). The measure of the SNA region (shaded) increases with ϵ, as does the range of the spectrum.

ing the minimum value that the Lyapunov exponent takes in the mth gap. We find empirically that $d_N \sim 1/N\epsilon^N$ [shown in Fig. 4(a) at $\epsilon=1$]. The behavior of the gap widths is more complicated and depends on the details of the Cayley tree. The widths are nonmonotonic as a function of gap index, but come in families: gaps belonging to a given family scale as a power, $w_N \sim 1/N^\theta$. The fastest decreasing are the Fibonacci gaps, $1,2,3,5,8,\ldots,F_k,\ldots$ ($\theta \equiv \theta_r \approx 2.3$), while the slowest is the family $1,4,17,\ldots,F_{1+3k}/2,\ldots$ ($\theta \equiv \theta_l \approx 1.88$): these are, respectively, the successive rightmost and leftmost nodes on the Cayley tree in Fig. 3 [see Fig. 4(b)]. Other families, which can be similarly defined on subtrees, also obey scaling, with exponents between θ_l and θ_r. When the gaps are ordered by rank r, then they scale as $w_r \sim 1/r^2$: this is consistent with the previously (numerically) obtained [3] gap distribution $\rho(s) \sim s^{-3/2}$, which has also been derived exactly through the Bethe ansatz [20].

Above ϵ_c, the states are exponentially localized and have the same localization length or Lyapunov exponent [4]. The gaps that dominate the spectrum at ϵ_c, persist for larger ϵ, but decrease in width according to the (empirical) scalings [see Fig. 4(b)],

$$w_N \sim \frac{1}{N^\theta \epsilon^{N-1}} \tag{5}$$

(where θ is particular to the family to which the gap belongs).

The dynamics of the Harper map corresponding to localized states is on SNAs [11], while that in the gaps continues to be on one-dimensional attractors similar to those below ϵ_c. However, since the gaps decrease in width, most of the dynamics is now on SNAs. By continuity, therefore, the SNA regions must start at each eigenvalue at ϵ_c, and widen gradually, since for large ϵ the spectrum lies in the range $0 \leqslant E \leqslant 2\epsilon$. A phase-diagram for this system in the E-ϵ plane is shown schematically in Fig. 5. The dynamics is entirely on fractal attractors with a negative Lyapunov exponent in the tonguelike regions, each of which starts at an eigenvalue at ϵ_c. The fractal (Cantor set) spectral structure is thus reflected in the hierarchically organized fractal ''tongues.''

The equivalence between the Harper equation and the Harper map thus provides a new mode of analysis of this problem which arises in numerous contexts [1–7]. The singular continuous nature of the eigenvalue spectrum, which has been the subject of considerable theoretical study, has been detected in experiments [21] as well, and therefore an understanding of the gap widths and their variation with energy and potential strength is of importance. The present technique gives a simple, but powerful method for the study of the spectrum to a finer level of detail than has hitherto been available. In this problem the details are *crucial*: although the spectrum of the Harper equation at ϵ_c is a Cantor set, the gaps may be labeled through a topological invariant of orbits of the Harper map that is related to previously de-

scribed rotation numbers for such systems [15] and to the integrated density of states [16]. The ordering of the gaps depends on number-theoretic properties of particular irrational frequency ω [17,19], while the gap indices determine the exponents for the scaling of gap widths as a function of potential strength. The phase diagram for the Harper system will consist of fractal tongues for all irrational frequencies ω, and in the tongues, the dynamics of the Harper map is on the SNAs. The ubiquity of such attractors and their correspondence with localized states further underscores their importance [11,12].

This research has been supported by the Department of Science and Technology, India. We have especially benefited from correspondence with Jean Bellisard.

[1] P.G. Harper, Proc. Phys. Soc., London, Sect. A **68**, 74 (1955).

[2] See e.g., D.R. Hofstadter, Phys. Rev. B **14**, 2259 (1976); J.B. Sokoloff, Phys. Rep. **126**, 189 (1985); M.Y. Azbel, P. Bak, and P.M. Chaikin, Phys. Rev. Lett. **59**, 926 (1987); H.–J. Stöckmann, in *Quantum Chaos, An Introduction* (Cambridge University Press, Cambridge, 1999), Chap. 4; P.B. Wiegmann, Suppl. Prog. Theor. Phys. **134**, 171 (1999); Y. Last, in *XI International Congress of Mathematical Physics, Paris, 1994*, edited by D. Iagolnitzer (International Press, Cambridge, MA, 1995), pp. 366–372; S. Jitomirskaya, *ibid.*, pp. 373–382.

[3] T. Geisel, R. Ketzmerick, and G. Petschel, in *Quantum Chaos*, edited by G. Casati and B. Chirikov (Cambridge University Press, Cambridge, 1995), pp. 633–660.

[4] G. André and S. Aubry, Ann. Isr. Phys. Soc. **3**, 133 (1980).

[5] J. Bellisard, R. Lima, and D. Testard, Commun. Math. Phys. **88**, 107 (1983).

[6] M. Kohmoto, Phys. Rev. Lett. **51**, 1198 (1983); M. Kohmoto, L.P. Kadanoff, and C. Tang, *ibid.* **50**, 1870 (1983); S. Ostlund, R. Pandit, D. Rand, H.J. Schellnhuber, and E.D. Siggia, *ibid.* **50**, 1873 (1983).

[7] S. Ostlund and R. Pandit, Phys. Rev. B **29**, 1394 (1984).

[8] J. Ketoja and I.I. Satija, Phys. Lett. A **194**, 64 (1994).

[9] J. Ketoja and I.I. Satija, Phys. Rev. Lett. **75**, 2762 (1995).

[10] H. Hiramoto and M. Kohmoto, Int. J. Mod. Phys. B **6**, 281 (1992).

[11] J. Ketoja and I.I. Satija, Physica D **109**, 70 (1997).

[12] A. Prasad, R. Ramaswamy, I.I. Satija, and N. Shah, Phys. Rev. Lett. **83**, 4530 (1999).

[13] C. Grebogi, E. Ott, S. Pelikan, and J. Yorke, Physica D **13**, 261 (1984); A. Prasad, S.S. Negi, and R. Ramaswamy, Int. J. Bifurcation Chaos Appl. Sci. Eng. **11**, 291 (2001).

[14] A. Bondeson, E. Ott, and T.M. Antonsen, Phys. Rev. Lett. **55**, 2103 (1985).

[15] The number N of *complete* traversals from $\tanh x=1$ to $\tanh x=-1$ is related to the winding number defined in R. Johnson and J. Moser, Commun. Math. Phys. **84**, 403 (1982); as $\Omega_N = M + N\omega$, M,N integer. See also, F. Delyon and B. Souillard, *ibid.* **89**, 415 (1983).

[16] J. Bellisard, in *From Number Theory to Physics*, edited by M. Waldschmidt, P. Moussa, J.-M. Luck, and C. Itzykson (Springer-Verlag, Berlin, 1992), pp. 538–630; J. Bellisard and B. Simon, J. Funct. Anal. **48**, 408 (1982).

[17] N.B. Slater, Proc. Cambridge Philos. Soc. **63**, 1115 (1967).

[18] A. Pandey, O. Bohigas, and M.-J. Giannoni, J. Phys. A **22**, 4083 (1989); A. Pandey and R. Ramaswamy, Phys. Rev. A **43**, 4237 (1991).

[19] The ordering function, Eq. (6) in [18] or the procedure leading to Eq. (33) in [17] applies to numbers $y_j=\{j\omega\}$ and needs slight modification in the present problem where, since we are considering only positive eigenvalues, the Ω_k's are constrained to lie in [1/2,1]. The details are given in S.S. Negi, Ph.D. thesis, Jawaharlal Nehru University, 2001.

[20] A.G. Abanov, J.C. Talstra, and P.B. Wiegmann, Nucl. Phys. B **525**, 571 (1998).

[21] C. Albrecht, J.H. Smet, K. von Klitzing, D. Weiss, V. Umansky, and H. Schweizer, Phys. Rev. Lett. **86**, 147 (2001).